© 2017. Published by The Company of Biologists Ltd | Development (2017) 144, 3134-3144 doi:10.1242/dev.149856

RESEARCH ARTICLE

Essential basal cytonemes take up Hedgehog in the *Drosophila* wing imaginal disc

Weitao Chen, Hai Huang, Ryo Hatori and Thomas B. Kornberg*

ABSTRACT

Morphogen concentration gradients that extend across developmental fields form by dispersion from source cells. In the *Drosophila* wing disc, Hedgehog (Hh) produced by posterior compartment cells distributes in a concentration gradient to adjacent cells of the anterior compartment. We monitored Hh:GFP after pulsed expression, and analyzed the movement and colocalization of Hh, Patched (Ptc) and Smoothened (Smo) proteins tagged with GFP or mCherry and expressed at physiological levels from bacterial artificial chromosome transgenes. Hh:GFP moved to basal subcellular locations prior to release from posterior compartment cells that express it, and was taken up by basal cytonemes that extend to the source cells. Hh and Ptc were present in puncta that moved along the basal cytonemes and formed characteristic apical-basal distributions in the anterior compartment cells. The basal cytonemes required *diaphanous*, *SCAR*, *Neuroglian* and *Synaptobrevin*, and both the Hh gradient and Hh signaling declined under conditions in which the cytonemes were compromised. These findings show that in the wing disc, Hh distributions and signaling are dependent upon basal release and uptake, and on cytoneme-mediated movement. No evidence for apical dispersion was obtained.

KEY WORDS: Hedgehog, Cytoneme, Patched, Smoothened, *Drosophila*

INTRODUCTION

The existence of molecular inducers (morphogens) that direct development and patterning was inferred more than 100 years ago from grafting experiments (Browne, 1909; Spemann and Mangold, 1924). Well-studied examples now include the Decapentaplegic (Dpp) and Hh proteins, which in the *Drosophila* wing imaginal disc distribute to form concentration gradients (Tabata and Takei, 2004). Dpp distributes from cells in a developmental organizer at the anterior (A)/posterior (P) compartment border, and Hh distributes from the P compartment, generating a gradient that extends over a distance of approximately 10 A compartment cells. The mechanism that disperses these proteins across their respective fields is the focus of this study.

Dispersion of Hh is evident from the distribution of antigen detected by antibody staining (Tabata and Kornberg, 1994; Taylor et al., 1993), and from the expression patterns of target genes that Hh signal transduction regulates (Strigini and Cohen, 1997). Among these regulated genes in the third instar wing disc is *ptc*, which is expressed in a band of approximately five to seven cells along the A/P border (Capdevila et al., 1994a; Mullor et al., 1997). Ptc is a Hh receptor (Lu et al., 2006; Marigo et al., 1996; Stone et al., 1996). *dpp*, another target, is expressed in a band of as many as five to six cells that is displaced from the border by approximately two to three cells (Raftery et al., 1991). Dpp also functions as a morphogen and disperses to form concentration gradients across both A and P compartments.

Reduced Hh signaling does not apparently directly affect the P cells that express it, but affects cells in which targets of Hh signaling are expressed (Strigini and Cohen, 1997). For example, both *ptc* and *dpp* expression decline under conditions of reduced Hh signaling, and the wings that develop have fewer cells in the region immediately anterior to the compartment border where *ptc* and *dpp* are expressed. Wing veins 3 and 4, which straddle the A/P border, are closer together than normal, and the anterior cross vein between veins 3 and 4 is frequently absent or malformed.

The 23 kD Hh protein has palmitate and cholesterol modifications that contribute to the high affinity of Hh for membranes (Pepinsky et al., 1998; Porter et al., 1996) and lipoprotein particles (Palm et al., 2013). Dispersion across A compartment cells must therefore involve a mechanism that accommodates its lipophilicity. It has been suggested that Hh is released from cells in a multimeric form, the conformation of which increases its hydrophilicity (Zeng et al., 2001). This model posits that the soluble multimer, either alone or complexed with chaperones, disperses in the extracellular milieu of the Hh-responding cells. There is, however, strong evidence for a direct transfer mechanism based on cytonemes that extend from the Hh-expressing cells in the P compartment (Bischoff et al., 2013; Callejo et al., 2011).

Cytonemes are specialized filopodia that link signal-producing and signal-receiving cells, and mediate the exchange and transport of signaling proteins (Kornberg and Roy, 2014). They protrude from many cell types, including the Dpp-receiving cells of the wing disc that have cytonemes that extend across the apical surface toward the Dpp-expressing cells at the A/P border (Hsiung et al., 2005; Ramirez-Weber and Kornberg, 1999; Roy et al., 2011). Disc cells also have cytonemes that extend from the basolateral membrane that have been implicated in Hh signaling (Callejo et al., 2011). These basolateral cytonemes mostly orient toward the A/P compartment border (Callejo et al., 2011; Roy et al., 2011), and some extend across the A/P border and appear to transport Hh to A compartment cells in motile puncta (Bilioni et al., 2013; Bischoff et al., 2013; Callejo et al., 2011).

The path that Hh takes prior to release at cytoneme tips is complex, initially involving placement in the apical membrane of Hh-producing cells, and dynamin-dependent endocytosis prior to transit to the basolateral compartment in a vesicular form (Callejo et al., 2011). The Hh-containing vesicles require the functions of Dispatched (Disp), Dally-like (Dlp) and Interference hedgehog

Cardiovascular Research Institute, University of California, San Francisco, CA 94143, USA.

*Author for correspondence (tkornberg@ucsf.edu)

W.C., 0000-0003-2049-6923; T.B.K., 0000-0002-6879-7066

Received 30 January 2017; Accepted 19 July 2017

Development (2017) 144, 3134-3144 doi:10.1242/dev.149856

(Ihog); without functional Disp, Dlp or Ihog, cells do not generate Hh-containing vesicles normally and do not release Hh. Little is known about the form of Hh when it transfers between cells at cytoneme points of contact, or the fate of Hh in A compartment cells. Although travel in exosomes has been proposed (Matusek et al., 2014), work from the Guerrero group suggests that Hh-containing vesicles that are associated with cytonemes may appear to be 'exosomes' if the cytonemes are not marked and simultaneously imaged (Gradilla et al., 2014).

The complex choreography that prepares Hh for delivery to A compartment cells was discovered in studies on Hh and Ihog, which were overexpressed as chimeras fused with either GFP or YFP (Bischoff et al., 2013; Callejo et al., 2011). These studies used the Gal4-UAS system, which elevates expression levels an estimated 10× (Yagi et al., 2010); the studies circumvented the cell lethality of Ihog overexpression with a time-limited pulse, and succeeded despite the apparent partial functionality of Hh:GFP expressed by this method (Torroja et al., 2004). In the work presented here, we build on these findings by analyzing Hh:GFP, Ptc:mCherry and Smo:GFP expressed by BAC transgenes. These constructs are regulated in the context of the normal gene sequences, and are fully functional. Histological characterizations both confirm the way Hh moves in producing cells, as discovered by Callejo et al. (2011), and show that motile puncta containing Hh and Ptc are present in cytonemes that protrude from the basal side of A compartment cells and extend across the A/P border. Hh moves together with Ptc in these cytonemes, and transport mediated by these cytonemes is required for Hh signaling and the Hh gradient. These findings provide direct visual and genetic evidence that basal cytonemes are essential conduits for Hh transport.

RESULTS

BAC transgenes that express fluorescent Hh, Ptc and Smo

To express active Hh:GFP, Ptc:mCherry and Smo:GFP at physiological levels, we generated BAC transgenes (see Materials and Methods). Each contains a genomic sequence that rescued apparent amorphs hh^{AC}, ptc^{16} or smo^{3}, respectively, and for each, flies with a single BAC-encoded allele were viable and had normal morphology. The distance between wing veins 3 and 4, a measure of Hh signaling (Mullor et al., 1997; Strigini and Cohen, 1997), was the same in control and experimental wings (Fig. 1A-D). GFP and mCherry fluorescence in embryo, larval, pupal and adult tissues that express the Hh, Ptc and Smo fusion proteins was detectable by confocal fluorescence microscopy, and the distributions of Hh:GFP, Ptc:mCherry and Smo:GFP conformed to descriptions reported for immunohistochemical staining, and for LacZ or GFP transgenes expressed under either *hh* or *ptc* enhancers (Fig. 1E, Fig. S1).

In third instar (L3) wing discs with Hh:GFP and Ptc:mCherry BACs, P compartment cells had green fluorescence that appeared to be membrane associated; levels of fluorescence in the wing pouch were elevated along the dorsal/ventral boundary, but were otherwise relatively uniform (Fig. 1E-G). Ptc:mCherry fluorescence was present in a strip of five to seven A compartment cells juxtaposed to the compartment border (Fig. 1E,F). Fluorescence was punctal, and numbers of puncta declined with increasing distance from the border. In a frontal optical plane near the basal surface, Hh:GFP was mostly membrane associated in the P compartment and punctal in the A compartment (Fig. 1H,H′). Many of these puncta had both green and red fluorescence (Fig. 1H′). The distribution of colocalized Hh:GFP and Ptc:mCherry is similar to the distribution of Hh and Ptc in wild-type discs stained with α-Hh and α-Ptc antibodies (Ramirez-Weber et al., 2000), and suggests that the BAC-encoded Hh:GFP moves basally from the cells in which it is expressed.

Fluorescence of BAC-encoded Hh:GFP was monitored in control discs and in discs that lacked *disp*, which encodes a function that is required by P compartment cells for Hh release (Burke et al., 1999). In control discs in which P compartment cells also express membrane-tethered mCherry, the P compartment-specific expression of Hh:GFP is apparent in a frontal, basolateral plane (Fig. 1I,J,K). GFP fluorescence was also present in puncta as far as eight cell diameters (~27 µm), and in membranes of cells within five to seven cells (~13 µm), of the border; levels of fluorescence declined with increasing distance from the border. By contrast, no GFP fluorescence was detected anterior to the border in discs that lacked *disp* function in the P compartment (Fig. 1L). Sagittal sections revealed that the absence of Disp also changed Hh:GFP localization in P cells. In normal, control discs, Hh:GFP was present both in cell membranes and puncta, (Fig. 1I′,J′,K′), but in P compartment cells lacking Disp, membrane-association of Hh:GFP was more uniform (Fig. 1L,L′). These distributions are consistent with those reported in published studies (Burke et al., 1999; Callejo et al., 2011).

Wing discs that coexpressed Ptc:mCherry and Smo:GFP had high levels of green fluorescence in P compartment cells and in adjacent A compartment cells that also express high levels of Ptc (Fig. 1M-P). Green fluorescence was lower in other A compartment cells. These patterns are consistent with immunohistochemical studies that reported elevated Smo levels in P compartment cells and in A cells adjacent to the A/P border (Denef et al., 2000). Smo:GFP fluorescence appeared to be membrane associated in both A and P compartment cells (Fig. 1P,P′).

Cytonemes project from Hh-receiving anterior cells into the posterior compartment

To better characterize the relative distributions of Hh:GFP and Ptc:mCherry, wing discs were analyzed at higher resolution and were imaged for periods of several minutes. The epithelial sheets of wing discs are not flat and develop complex folds during L3. Although discs that have been flattened under cover slips generate higher resolution images, flattening damages sensitive structures such as cytonemes and potentially compromises spatial relationships of cell constituents. To image unflattened discs, we mounted discs in hanging drops and analyzed two types of preparation (Fig. 2A). Owing to the concavity of the pouch region in late L3 discs, we limited studies of the pouch cells to early L3 discs, which are relatively flat, and limited analysis of late L3 discs to the wing hinge primordium, which is also relatively flat.

Fig. 2B,C show images of the pouch region of an unfixed wing disc from early L3 that expressed Ptc:mCherry. Many fluorescent Ptc puncta were present in the A compartment; most were near the compartment border. Fluorescent Ptc puncta (mean, 70; n=5 discs) were also present in the P compartment, with some as far as 30 µm from the border, although >50% were within 10 µm (Fig. 2D). The concentration gradient of puncta in the P compartment is quantified in Fig. 2D. The sagittal projection image (Fig. 2C) reveals the polarized apicobasal distribution of Ptc:mCherry puncta. The thickness of the pouch region was ~30-35 µm; >50% of Ptc:mCherry puncta were within 5 µm of the basal surface, and ~80% were within 10 µm (Fig. 2C,E). No fluorescent Ptc puncta were observed at apical optical planes in the P compartment. The basal Ptc puncta were motile, and in a 30 µm segment along the A/P axis; approximately two puncta crossed the compartment border from the A side per minute.

Development (2017) 144, 3134-3144 doi:10.1242/dev.149856

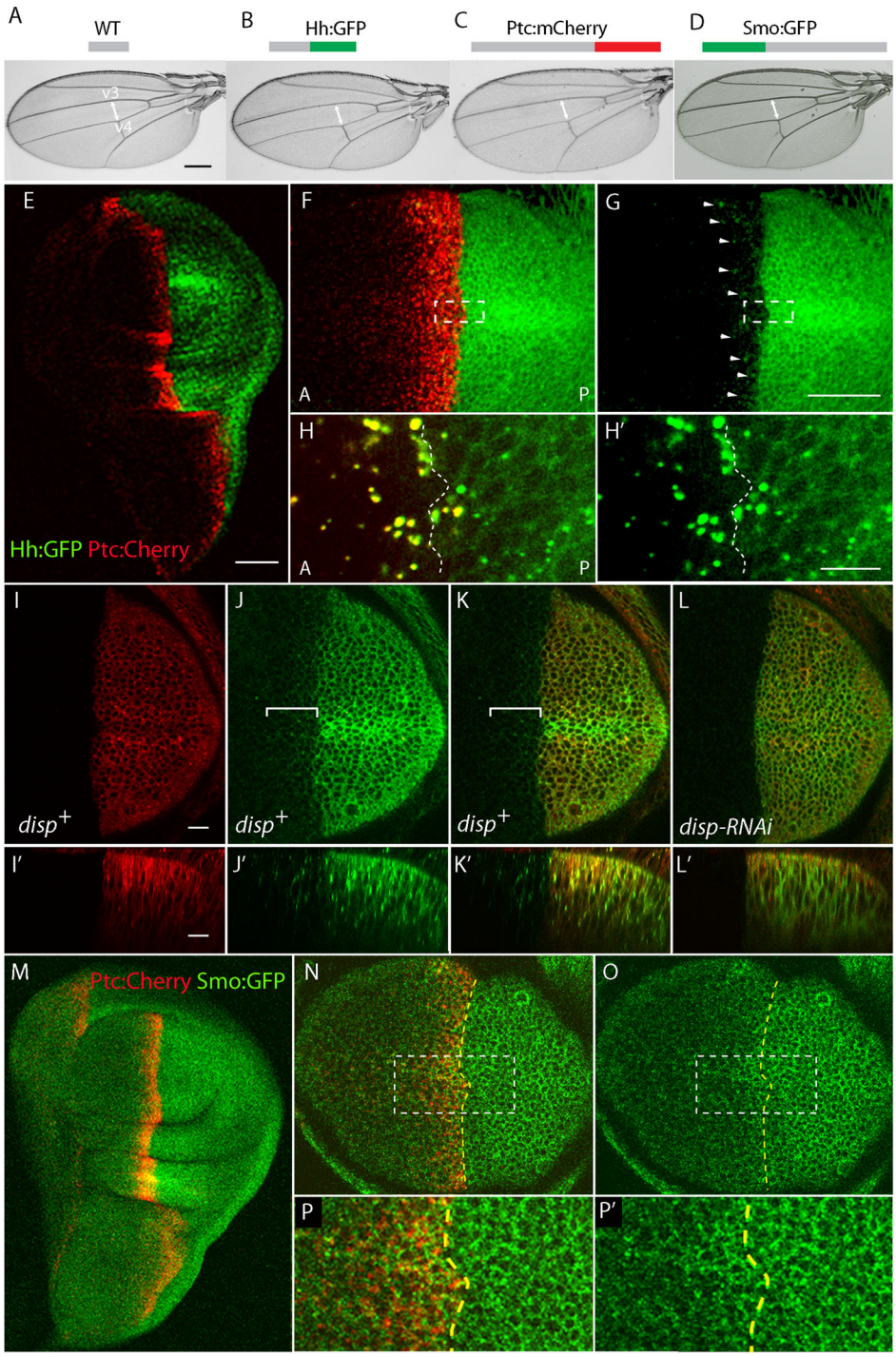

Fig. 1. Distributions of Hh, Ptc and Smo tagged with fluorescent proteins and expressed from BAC transgenes. (A-D) Diagrams illustrating the approximate locations of GFP and mCherry tags, and (below) micrographs of wings of control (*yw*) (A), *hh* null (hh^{AC}/hh^{AC}) with Hh:GFP BAC (B), *ptc* null (ptc^{16}/ptc^{16}) with Ptc:mCherry BAC (C) and smo^{3}/smo^{3} with Smo:GFP BAC (D). The distances between veins 3 and 4 were indistinguishable in control and mutant wings. (E-P′) BAC-encoded Hh:GFP, Ptc:mCherry and Smo:GFP in wing discs. (E-G) Distributions of Ptc:mCherry and Hh:GFP conform to compartment-specific expression patterns of respective endogenous genes (Capdevila et al., 1994b; Tabata and Kornberg, 1994). Most Hh:GFP is in the P compartment, but some (G, arrowheads, *Z* projection image) is in the Ptc domain (F, green channel only). (H,H′) Higher magnification images of basal optical sections of the boxed areas in F and G. The A/P compartment border is indicated by dashed lines (H, green channel; H′, green+red channel showing colocalization of Hh:GFP and Ptc:mCherry in puncta, mostly in the A compartment). (I-L) BAC-encoded Hh:GFP with the P compartment marked by mCherry (*hh*-Gal4 *UAS*-CD8:mCherry), $disp^{+}$ (I,J,K) or depleted for *disp* (*hh*-Gal4 *UAS*-*disp*-RNAi) (L,L′) (I, red channel; J, green channel; K,L, merge). (J,K) Brackets indicate Hh:GFP in the A compartment. (I′,J′,K′,L′) Sagittal projections of I, J, K and L. (M-P) Elevated levels of Smo:GFP in the P compartment and *ptc* domain (O,P′, green channel; M,N,P, merge). (N-P′) Higher magnification images of M; the dashed line marks the A/P compartment border. (P,P′) Higher magnification images of the boxed areas in N and O reveal similar subcellular Smo:GFP distributions in A and P cells. All discs in all figures are from late L3 unless indicated; anterior, left; sagittal projections, apical up. Scale bars: 200 µm in A; 40 µm in E and G; 10 µm in H′, I and I′.

To further characterize the fluorescent Ptc puncta, we examined late L3 discs that had A cells with membranes marked with membrane-tethered GFP (*ptc*>Gal4 *UAS*>CD8:GFP) and P cells with nuclei marked with DsRed (*hh*-nlsDsRed). At a basolateral optical plane, GFP and DsRed fluorescence was restricted to the A and P compartments, respectively (Fig. 2F), and the juxtaposition of green and red fluorescence appeared to define the A/P boundary. However, at the basal surface, GFP fluorescence was not restricted to the A compartment, but extended 2-20 µm into the P compartment. Cellular extensions could be resolved at the most posterior regions of the GFP fluorescence (Fig. 2F′). Fig. 2F″ displays a sagittal view in which these fluorescent protrusions are apparent extending from the A compartment along the basal surface of adjacent P compartment cells. The appearance of these protrusions suggests that they may be basal cytonemes that have roles in Hh signaling (Bischoff et al., 2013; Callejo et al., 2011).

The basal protrusions were mostly perpendicular to the A/P compartment border. Although some were static, most were dynamic, with rates of extension and retraction measured as 0.15±0.03 µm/s and 0.12±0.02 µm/s, respectively (Fig. 2G,G′, Movie 1). These rates are comparable to rates of filopodia extension and retraction reported for the thin filopodia of sea urchin embryos (Miller et al., 1995). To determine whether there is a correlation between the presence of Ptc:mCherry puncta posterior to the

Development (2017) 144, 3134-3144 doi:10.1242/dev.149856

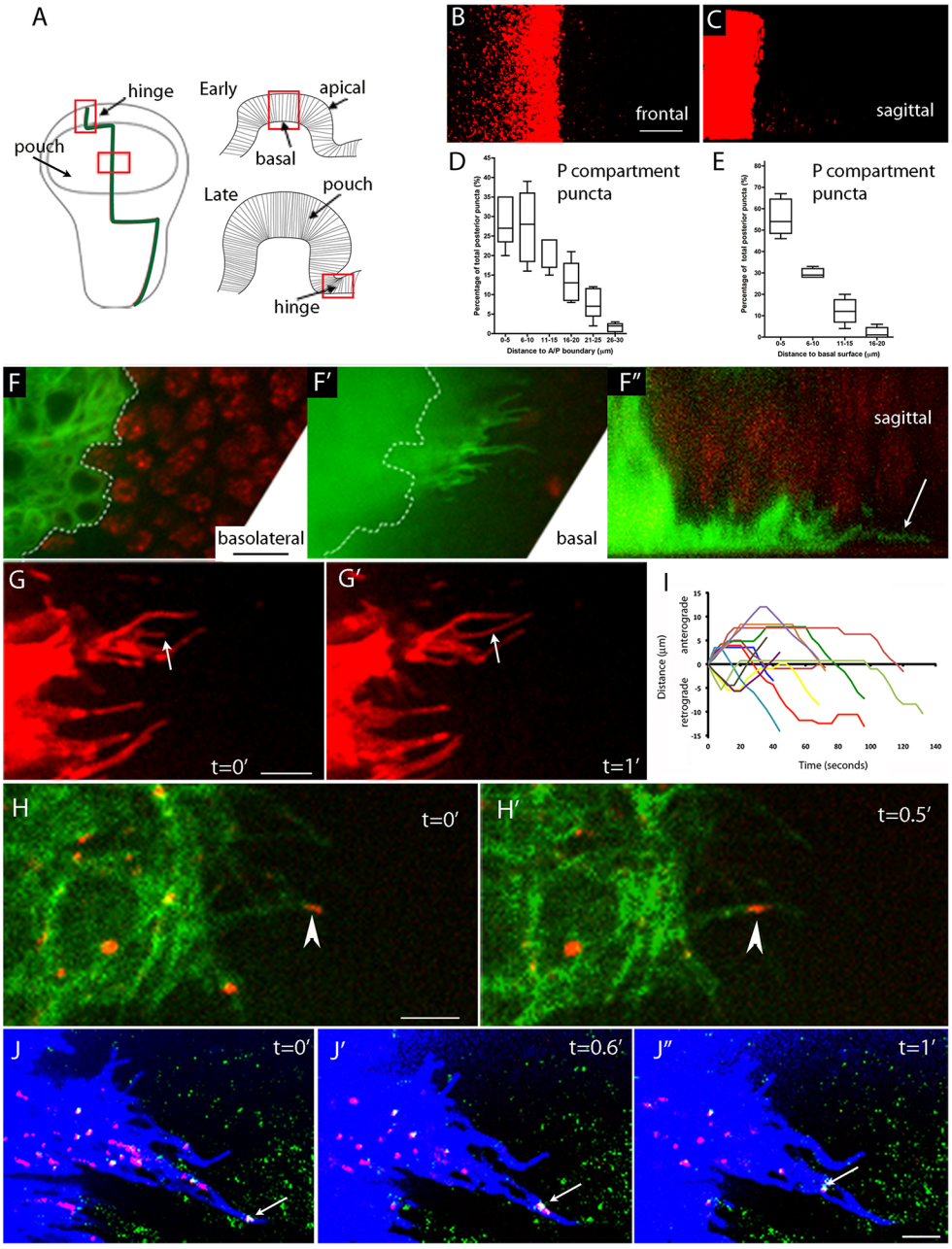

Fig. 2. Basal cytonemes at the A/P compartment border. (A) Left: line drawing of a wing disc viewed from the columnar epithelium basal side. The green line indicates the A/P border; boxes mark the hinge (upper) and pouch (lower). Right: transverse sections showing the concavity of the pouch in early and late L3 discs. (B,C) Frontal (B) and sagittal (C) optical projections of the pouch region of an unfixed early L3 disc expressing BAC-encoded Ptc:mCherry. Ptc:mCherry puncta were present in the A compartment, mostly near the compartment border; Ptc:mCherry puncta were also present in the P compartment. (D,E) Quantification of Ptc:mCherry puncta along anteroposterior (D, *n*=5 discs) and apicobasal (E, *n*=5 discs) axes in the P compartment (standard box plot and whisker diagrams based on minimum, first quartile, median, third quartile and maximum values; 'whiskers' show minima and maxima). (F-F″) Frontal sections (F,F′) and sagittal projection (F″) of the hinge region, showing membrane-marked A cells (*ptc*-Gal4 *UAS*-CD8:GFP) and marked P cells (*hh*-nlsDsRed). A cell cytonemes (dashed line) project along the basal surface. (G,G′,H,H′) Hinge region, with marked membranes of A cells (*ptc*-Gal4 *UAS*-CD8:mCherry; G,G′) and BAC-encoded Ptc:mCherry (H,H′). Arrows indicate motile cytonemes (G,G′); arrowheads indicate motile Ptc:mCherry-containing puncta (H,H′). (I) Kymograph describing the movement of 12 Ptc:mCherry-containing puncta. (J-J″) Motile puncta with fluorescent BAC-expressed Ptc:mCherry and Hh:GFP in A compartment, and A compartment marked cytonemes (*ptc*-Gal4 *UAS*-CD4:IFP2.0). Data set: 922 cytonemes in a 50×50 µm area of the ventral hinge region (*n*=25 discs); 133 cytonemes had 386 Ptc:mCherry puncta, 114 of which also had Hh:GFP; 789 cytonemes had neither Ptc:mCherry nor Hh:GFP puncta. Scale bars: 10 µm in B; 5 µm in F, G, H and J′′.

compartment border and the presence of the cross-border basal cytonemes, we examined disc preparations in which A compartment cells had membranes marked with GFP (*ptc*>Gal4 *UAS*>CD8:GFP) and also expressed Ptc:mCherry. The Ptc:mCherry puncta appeared to travel along the cytonemes that track on the basal surface of the disc, both within the A compartment and across the compartment border. Images of the cytomemes that project into the P compartment showed that some were populated by fluorescent Ptc puncta (Fig. 2H). Although these images did not resolve whether Ptc:mCherry puncta were inside or on the surface of the cytonemes, the puncta could be monitored for movement (Fig. 2H,H′,I, Movie 2). Puncta moved in both anterograde and retrograde directions and at a similar rate (~0.4 µm/s), with periods of movement ≤40 s. There were also periods of apparent stalling, and although we do not understand the significance of the intermittent motion, the fact that puncta moved linearly with a consistent velocity in the range of known actin-based myosin motors (Mehta et al., 1999) strongly suggests that cytoneme-mediated movement of Ptc is motor dependent.

Cytonemes of Hh-responding cells transport Hh

We tracked BAC-encoded Hh:GFP and Ptc:mCherry in wing discs that expressed membrane-tethered infrared fluorescent protein (Yu et al., 2014) in the *ptc* expression domain (*ptc*-Gal4 UAS-IFP2.0). Cytonemes extending from A compartment cells were detected by their infrared fluorescence (Fig. 2J). Many puncta with bright GFP and mCherry fluorescence were detected in A and P cells, respectively, and although most of the Hh:GFP puncta were in P compartment cells, some were in A cells, and some colocalized with cytonemes that extended into the P compartment. We also detected motile puncta that had both green and red fluorescence in cytonemes and in A compartment cells (Fig. 2J-J″, Movie 3). Not all cytonemes

Development (2017) 144, 3134-3144 doi:10.1242/dev.149856

had Ptc:mCherry puncta, but Hh:GFP puncta were only detected in the cytonemes that did. These results suggest that cytonemes extending from A compartment cells can pick up Hh from P cells, and that Hh associated with Ptc is present in these cytonemes.

The Hh concentration gradient and Hh function require cytoneme-mediated transport

To assess the role of the basal A compartment cytonemes in Hh signaling, we monitored signaling and cytonemes in mutant genotypes that have been previously shown to impair cytonemes and cytoneme-mediated signaling. Expression of *diaphanous* (*dia*) RNAi and *Neuroglian* (*Nrg*) RNAi in tracheal cells (Roy et al., 2014), and expression of *SCAR* RNAi in P compartment disc cells (Bischoff et al., 2013), reduce cytoneme number and length as well as signaling in tracheal and disc cells, respectively. We expressed *dia* RNAi, *SCAR* RNAi and *Nrg* RNAi in the *ptc* domain (*ptc*-Gal4 *tub*-Gal80^{ts} and either *UAS-dia* RNAi, *UAS-SCAR* RNAi or *UAS-Nrg* RNAi), and marked cytonemes by expressing a membrane-tethered fluorescent protein (*UAS*-CD8:mCherry or *UAS*-CD8:GFP). As shown in Fig. 3, expression of the *dia* and *SCAR* RNAi constructs in A compartment cells reduced Hh:GFP fluorescence and Ptc levels in A compartment cells (Fig. 3A-G,O, P,R) and reduced the number and length of A compartment cytonemes (Fig. 3H-J,M,N). No changes to cell lethality or apicobasal organization in the RNAi-expressing cells were detected (Fig. S2). Expression of *Nrg* RNAi in A compartment cells reduced Ptc levels (Fig. 3O,T), and reduced the number and length of A compartment cytonemes (Fig. 3H,K,M,N).

We also investigated whether the v-SNARE Synaptobrevin (Syb) is required for cytoneme-mediated signaling because of its role in vesicle transport and fusion, and because of the vesicular state of Hh as it is prepared for release from P compartment cells. The *Drosophila* genome encodes two Syb homologs. Although neuronal Synaptobrevin (nSyb) is expressed exclusively in

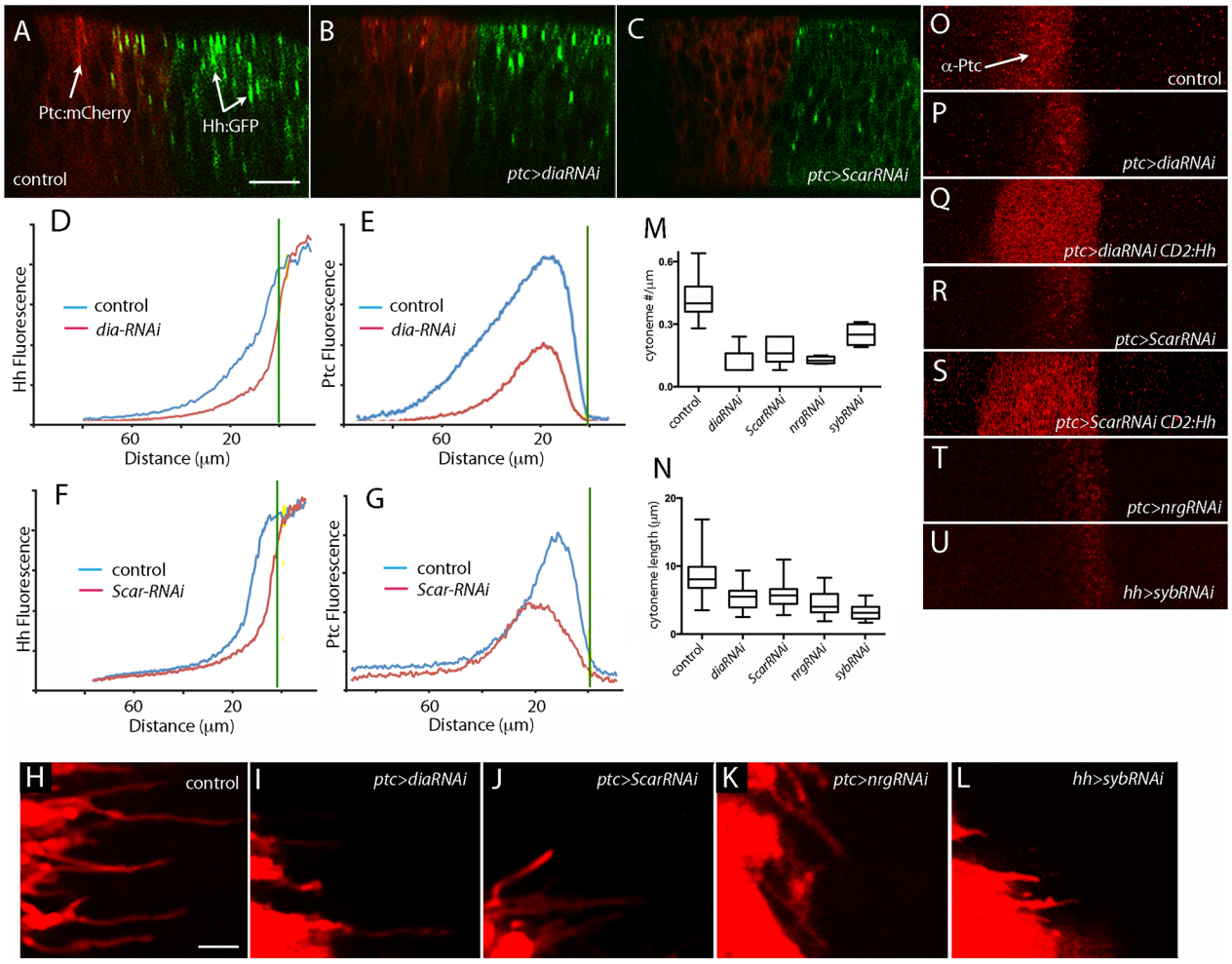

Fig. 3. Cytoneme transport is required for Hh dispersion and signaling. (A-G) Sagittal (A-C) images of L3 wing pouch, BAC-expressed Ptc:mCherry and Hh:GFP. The spread of Hh:GFP into A cells and Ptc levels was reduced by *dia* RNAi (*ptc*-Gal4 *UAS-dia* RNAi) (B,D,E) and *SCAR* RNAi (*ptc*-Gal4 *UAS-SCAR* RNAi) (C,F,G) in the *ptc* domain. (H-N) A compartment cytonemes marked with CD8:mCherry or CD8:GFP were shorter and less abundant under conditions of *dia* (I), *SCAR* (J) and *Nrg* (K) depletion in the *ptc* domain (*ptc*-Gal4), and under conditions of *Syb* depletion (L) in the P compartment (*hh*-Gal4, *UAS-Syb* RNAi *dpp*-LexA *lexO*-mCherryCAAX). (M,N) Standard box plot and whisker diagrams based on minimum, first quartile, median, third quartile and maximum values; 'whiskers' show minima and maxima. *P*-values (*t*-test), n=8 for all genotypes: control and *dia* RNAi-treated length (P=5.8E-08) and number comparisons (P=0.00025); control and *SCAR* RNAi-treated length (P=8.87E-08) and number comparisons (P=0.00042). *SCAR* RNAi- and *dia* RNAi-treated length (P=0.32) and number comparisons (P=0.50); control and *Syb* RNAi-treated length (P=8.92E-17) and number comparisons (P=0.0018); control and *Nrg* RNAi-treated length (P=1.28E-11) and number comparisons (P=0.00054). (O-U) α-Ptc staining at the wing pouch A/P compartment border for control (O), *dia*-depleted (P), *SCAR*-depleted (R), *Nrg*-depleted (T) and *Syb*-depleted (U) discs. Hh:CD2 reverses the effects of *dia* RNAi and *SCAR* RNAi on Ptc (Q,S). Scale bars: 10 μm in A; 5 μm in H.

Development (2017) 144, 3134-3144 doi:10.1242/dev.149856

neurons (DiAntonio et al., 1993), and Syb is ubiquitously expressed and has a general role in membrane trafficking (Chin et al., 1993), the two SNAREs appear to be functionally interchangeable (Bhattacharya et al., 2002). Syb has been shown to play a role in Wingless signaling in wing imaginal discs (Yamazaki et al., 2016). Expression of *Syb* RNAi in the A compartment (*ptc*-Gal4 *UAS-Syb* RNAi *UAS*-CD8:mCherry) had no apparent effect (not shown), but in the P compartment, *Syb* RNAi expression (*hh*-Gal4 *UAS-Syb* RNAi and *dpp*-LexA *lexO*-mCherryCAAX) reduced Ptc in A compartment cells and reduced the number and length of A cytonemes at the compartment border (Fig. 3H,L-N,O,U). This result suggests that A compartment cytonemes do not function normally if vesicle transport in the cells they contact and synapse with is compromised.

Features of the cuticle of the adult thorax that fail to develop normally under conditions of abnormal Hh signaling include the number of wing cells between wing veins 3 and 4, which decreases under conditions of reduced Hh signaling and increases under conditions of increased signaling (Mullor et al., 1997; Strigini and Cohen, 1997). *dia* RNAi and *SCAR* RNAi expression in the *ptc* domain significantly decreased the intervein 3-4 width and affected the anterior cross-vein (Fig. S3A-C,G). In wings with reduced Dia, the cell density in the 3-4 intervein region was also reduced (Fig. S3B). Although other regions and structures of the wings were not apparently affected, *SCAR* RNAi expression in the *ptc* domain reduced the size of the scutellum and eliminated the four scutellar bristles (Fig. S3H,I).

To determine if cells deficient for Dia or SCAR are competent for Hh signal transduction despite their inability to take up Hh from P compartment Hh-expressing cells, we expressed a membrane-tethered form of Hh (CD2:Hh) together with *dia* RNAi or *SCAR* RNAi. CD2:Hh is active but does not signal efficiently at long range and does not disperse at normal levels (Strigini and Cohen, 1997). Expression of CD2:Hh in the *ptc* domain increased levels of Ptc (Fig. 3Q,S), and rescued the 3-4 intervein region phenotypes of *dia* RNAi and *SCAR* RNAi (Fig. S3E-G). Expression of CD2:Hh restored the scutellum morphology and the scutellar bristles (Fig. S3J). We conclude that the A compartment cytonemes that take up Hh are required for the dispersal of Hh that forms the Hh concentration gradient in the wing disc. Note that expression of CD2:Hh increased Ptc above normal levels, presumably a consequence of positive feedback. The number of Ptc fluorescent puncta in the P compartment also increased, but we could not resolve whether these dots are background or a consequence, perhaps, of an associated increase in the number of cytonemes that these cells extend.

Cell-cell contacts at the A/P compartment border

We used the GRASP technique (GFP Reconstitution Across Synaptic Partners) (Feinberg et al., 2008; Gordon and Scott, 2009) to image contacts that cells make at the A/P compartment border. We expressed CD4:GFP^{11} (transmembrane domain of mouse lymphocyte protein CD4 fused with a GFP fragment that includes the 11th strand of the 11-stranded photocenter) in the *dpp* domain (*dpp*-LexA *lexO*-CD4:GFP^{11}), and expressed CD4:GFP$^{1-10}$ (a fusion with a fragment that includes GFP photocenter strands 1-10) in the P compartment (*hh*-Gal4 *UAS*-CD4:GFP$^{1-10}$). Expression of mCherry marked the membranes of either A (*dpp*>LexA *lexO*-mCherryCAAX) or P (*hh*-Gal4 *UAS*-CD8:mCherry) cells, and although the membrane-tethered GFP fragments are not themselves fluorescent, reconstitution of GFP generates fluorescence at points of cell-cell contact (Fig. 4).

We detected GFP fluorescence in discs in which A cells at the compartment border expressed GFP^{11} and P cells expressed GFP$^{1-10}$. Fluorescence was present in a thin strip along the apicobasal axis at the apparent juxtaposition of the A and P compartments, and more broadly at the basal surface (Fig. 4A,B). Fluorescent cytonemes were detected at the basal surface extending in both anterior and posterior directions as far as 15-20 µm. By locating the approximate position of the compartment border with α-Ptc antibody staining (Fig. 4D,E), we estimated that the fluorescence intensity profile is roughly symmetric to either side of the compartment border. GRASP fluorescence appeared to mark the entire length of the cytonemes. In addition to the GRASP-marked cytonemes, cytonemes were present that were marked by mCherry, but not GFP, fluorescence (Fig. 4D); their relative mCherry fluorescence in successive apicobasal optical planes suggested that they were more basal than the GRASP-marked cytonemes and, therefore, might not track along the basal cell surfaces. Points of GFP fluorescence were also observed in basolateral optical planes (Fig. 4A′-A‴); their lack of association with GRASP-marked extensions might indicate that cytonemes in the basolateral region do not track in the same manner as the basal cytonemes, that they have lower fluorescence or greater curvature, or that they are more sensitive to breakage and to the manipulations that were used to prepare the discs for imaging. Although we cannot dismiss the possibility that these points of fluorescence are free exosomes (Gradilla et al., 2014; Matusek et al., 2014), we favor the idea that they are puncta associated with unmarked cytonemes. Fig. 4F shows GRASP fluorescence for Syb:GFP$^{1-10}$ expressed in P compartment cells, suggesting that the cytoneme-mediated, Syb-dependent signaling (Fig. 3H-J,Q) is contact dependent, and that one of the subcellular destinations of Syb in Hh-expressing cells may be the synapse from which Hh is released and translocates to the receiving cell.

Intracellular Hh routes in producing and receiving cells

The discovery of the multi-stage intracellular route that Hh takes prior to its release from producing cells (Callejo et al., 2011) showed that newly synthesized Hh first moves to the apical membrane, and that it is encapsulated in endocytic vesicles that translocate to basolateral and basal cytonemes. We investigated the intracellular movement of Hh further by taking advantage of tools that we developed to characterize fluorescent proteins.

Because Hh protein moves from cells in the P compartment that produce it, the source of Hh that is detected in steady-state preparations of discs is uncertain. For example, the panels in Fig. 5A,B show frontal and sagittal sections of the pouch region from a wing disc that expressed BAC-encoded Hh:GFP and has a clone in the P compartment with ∼40 cells that lack the transgene. Hh:GFP is present and distributed in the apicobasal axis of the normal P compartment cells, but it is not absent from the region of the clone. Hh levels are significantly reduced and, in contrast to normal cells, Hh:GFP is strongly biased to the basal side of clone cells. We suggest that this Hh:GFP was produced by neighboring cells, and that it is in the region of the clone because of movement along basal and basolateral cytonemes. The images do not distinguish whether Hh:GFP in the region of the clones is inside or outside the mutant cells; we assume that it is outside (and cytoneme associated).

To better characterize how Hh moves in P cells that make it and A cells that receive it, we examined the distribution of Hh:GFP produced during a time-limited pulse. The panels in Fig. 5C show sagittal and frontal sections of the pouch region of a wing disc that

Development (2017) 144, 3134-3144 doi:10.1242/dev.149856

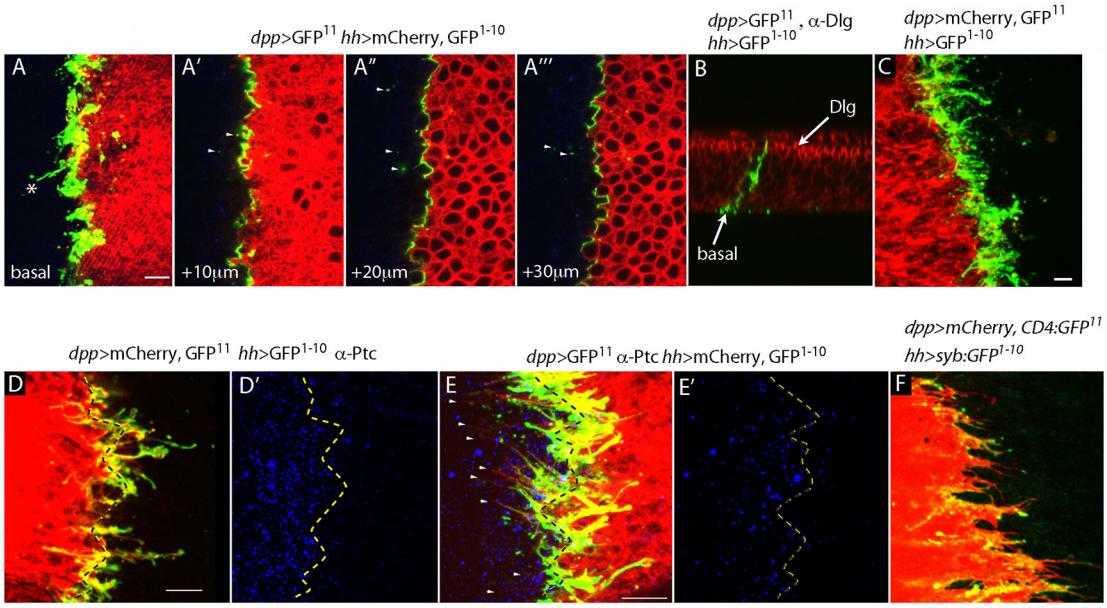

Fig. 4. Cytonemes extend direct contacts across the A/P compartment border. (A-A‴) Optical sections at basal (A) and more apical elevations of unfixed disc (A′-A‴) with the P compartment marked with mCherry (*hh*-Gal4 *UAS*-CD8:mCherry), membrane-tethered GFP^{11} in the *dpp* domain (*dpp*-LexA *lexO*-CD4:GFP^{11}), and membrane-tethered GFP$^{1-10}$ in the P compartment (*hh*-Gal4 *UAS*-CD4:GFP$^{1-10}$). GRASP marked the juxtaposition of A and P compartments at basolateral elevations, and broader domain and cellular projections (asterisk) at the basal surface. Arrowheads indicate GRASP displaced from the border in more apical sections (A,A′,A‴). (B) Sagittal image of disc fixed and stained with α-Dlg antibody and with GRASP fluorescence (*dpp*-LexA *lexO*-CD4:GFP^{11} *hh*-Gal4 *UAS*-CD4:GFP$^{1-10}$) that extends basolaterally and along the basal surface (arrow). (C) GRASP fluorescence of an unfixed disc with the A compartment marked with mCherry (*dpp*-LexA *lexO*-CD4:GFP^{11} *lexO*-mCherryCAAX *hh*-Gal4 *UAS*-CD4:GFP$^{1-10}$). (D,E) GRASP fluorescence of fixed discs with the A/P compartment border identified by α-Ptc (blue) staining and marked with dashed lines. Arrowheads in E indicate cytonemes lacking GRASP fluorescence. (D,D′) Genotype: *dpp*-LexA *lexO*-CD4:GFP^{11} *lexO*-mCherryCAAX *hh*-Gal4 *UAS*-CD4:GFP$^{1-10}$; (E,E′) genotype: *dpp*-LexA *lexO*-CD4:GFP^{11} *hh*-Gal4 *UAS*-CD4:GFP$^{1-10}$ *UAS*-CD8:mCherry. (F) GRASP fluorescence with membrane-tethered GFP^{11} in A compartment cells marked with mCherry and Syb-tethered GFP$^{1-10}$ in P compartment cells (*dpp*-LexA *lexO*-CD4:GFP^{11} *lexO*-mCherryCAAX *hh*-Gal4 *UAS*-Syb:GFP$^{1-10}$). Scale bars: 5 μm in A, D and E; 10 μm in C.

expressed Hh:GFP for 8-16 h. At 8 h, most fluorescence in the P compartment was apical, and fluorescence was not detected in A compartment border cells. However, fluorescence in the basolateral and basal portions of the P cells increased with longer times of expression, and appeared to be uniform in intensity along the apicobasal axis at 14-16 h. Fluorescence in the A border cells also increased, and was significantly greater at and near the basal surface (Fig. 5D). These distributions are consistent with the Guerrero group's model of basal dispersion (Callejo et al., 2011).

To better resolve the apicobasal distribution of Hh in A and P cells, we imaged Hh:GFP and stained with α-Cad and α-Dlg antibodies to delineate the apical domain of the columnar disc cells. Cad and Dlg are components of the adherens and septate junctions, respectively. In the P compartment, Hh:GFP was present throughout the basolateral membranes, and was prominent in the apical band that stained for Cad (Fig. 6A). This apical accumulation of Hh:GFP partially overlapped with the band of Dlg staining (Fig. 6B). In the A compartment cells at the border, Hh:GFP fluorescence was basal and basolateral, and was also detected coincident with the Dlg domain.

To relate these distributions to Ptc and Smo, we also imaged Ptc:mCherry and Smo:GFP (Fig. 6C,D). Ptc:mCherry colocalized with Hh:GFP to the anterior side of the A/P border and distributed over most of the apicobasal axis (Fig. 6B,D). Neither Ptc:mCherry nor Hh:GFP was detected apical to the Dlg-staining domain. Ptc:mCherry and Smo:GFP did not appear to colocalize (Fig. 6D). Levels of Smo were higher in P cells and in A cells adjacent to the border, and were lower in more anterior cells (Fig. 1M-P′ and Fig. 6D). In both A and P cells, fluorescent Smo puncta were present in the membranes extending apically to the Dlg domain (Fig. 6D). These distributions suggest that Hh movement in A cells involves direct association with Ptc, and with basal uptake and apical translocation. The distribution of Smo strongly correlated with the presence of Hh, and was high in both A and P cells that have Hh, and low in A cells that lack Hh.

DISCUSSION

Two striking aspects of Hh signaling evident in the images presented in this paper are the elaborate choreography that directs Hh to its destination in receiving cells (Fig. 5), and the spatial and quantitative regulation of Ptc and Smo (Figs 1 and 2). These features make it essential to use sensitive methods to precisely monitor the components of Hh signaling at physiological levels in tissues that are minimally disturbed. The BAC-encoded, fluorescent protein chimeras of Hh, Ptc and Smo we characterized in unflattened wing discs address this imperative, and open the analysis of morphogen distribution to real-time imaging of fully functional morphogens. We show that Hh dispersion is dependent on cytonemes that extend from the basal surface of A cells and that move Hh from P cells that express it to A cells that activate signal transduction. The distinctive subcellular distributions of Hh, Ptc and Smo suggest that after Hh is transported to the basal and basolateral membranes of P compartment cells for release, and after uptake, Hh is transported apically by A compartment cells for processing and signal transduction.

Direct imaging of functional Hh protein

A variety of direct imaging approaches have been used with recombinant fluorescent protein-morphogen chimeras. Spatially localized expression has been achieved by electroporation of

Development (2017) 144, 3134-3144 doi:10.1242/dev.149856

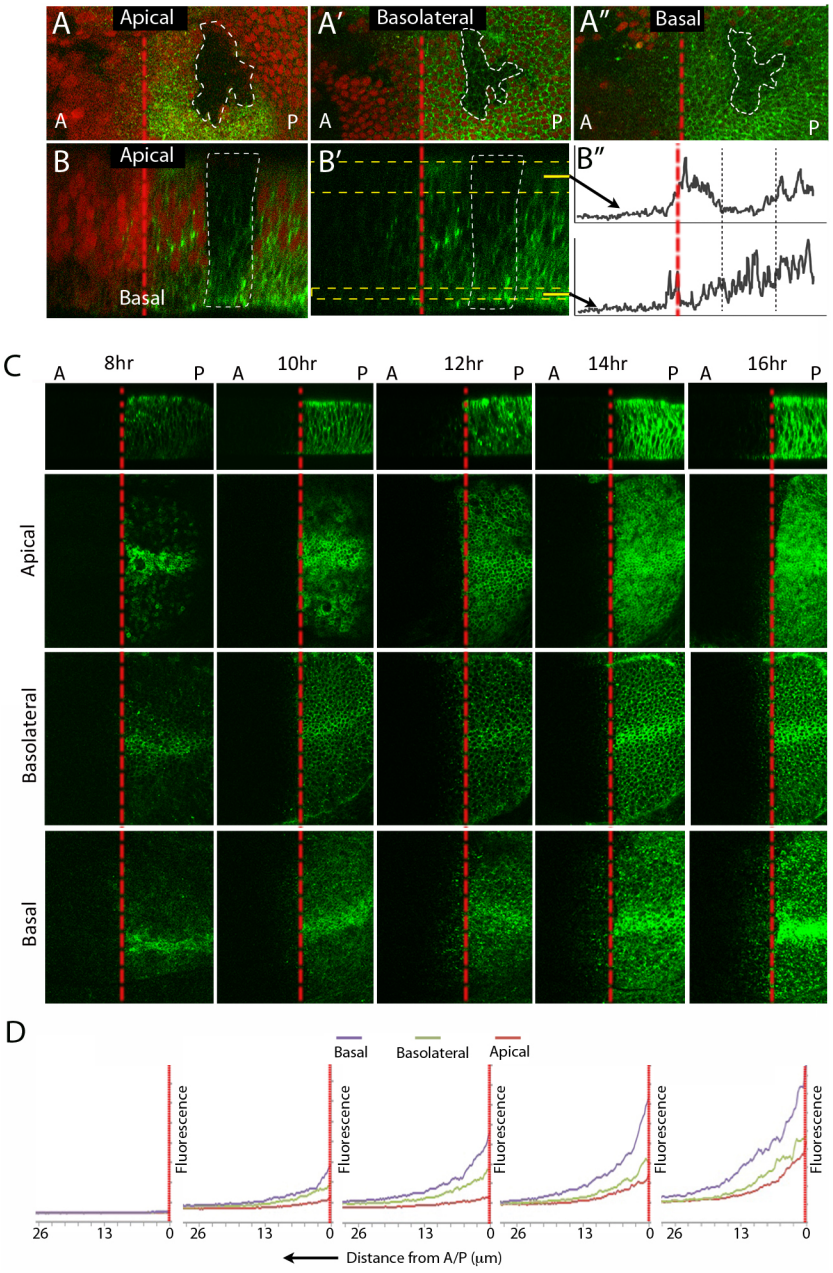

Fig. 5. Hh dispersion in the A and P compartments. (A-B′) BAC-encoded Hh:GFP and Ptc:mCherry at frontal (A-A″) and sagittal (B-B′) planes. White dashed lines surround a clone lacking Hh:GFP BAC; red dashed lines indicate the A/P compartment border. GFP fluorescence is reduced in the clone except at the basal surface. (B″) GFP fluorescence intensity in regions bounded by the yellow dashed lines in B′ at the indicated planes. (C,D) Frontal images showing Hh:GFP expressed by the transgene (*hh*-Gal4 *tub*-Gal80^{ts} *UAS*-Hh:GFP) following a shift to 29°C. Red dashed lines indicate the A/P compartment border. The subcellular localization of Hh:GFP in the P compartment was mostly apical at 8 h, and more basal later. The localization of Hh:GFP in A compartment cells was mostly basal at 12 h and spread more apical later. (D) Graphical representation of Hh:GFP fluorescence at the indicated planes.

cDNAs into living embryos (Sanders et al., 2013; Toyoda et al., 2010), by injection of *in vitro*-synthesized mRNAs into embryos (Muller et al., 2012), and from transgenes under heterologous regulation such as the Gal4-UAS system (Callejo et al., 2011; Kicheva et al., 2007; Zhou et al., 2012). Protein dispersing from expressing cells has been detected by fluorescent imaging, but because expression at an ectopic site can have unforeseen consequences if the systems that normally process and release the morphogen are overwhelmed, or if subcellular structures that are involved are influenced by expression levels, even these direct measures can be problematic in contexts of overexpression and abnormal regulation. The critical metric is function.

The BAC-encoded Hh:GFP, Ptc:mCherry and Smo:GFP fully rescue respective genetic nulls. We could not detect abnormalities in rescued flies, and therefore dispense with concerns about either aberrant activity of the protein chimeras or abnormal regulation of their expression, processing and dispersion. The 173-residue Hh moiety of chimeric protein comprises only 35% of Hh:GFP, yet its dispersion and capacity to bind receptor and activate signal transduction are not significantly impaired, and its activity is not significantly reduced. It is also impressive that confocal microscopy is now sufficiently sensitive to detect fusion proteins expressed at normal physiological levels.

Cytonemes take up and transport Hh protein in the wing disc

We found that cells at the wing disc A/P border extend basal cytonemes that take up Hh from P cells, and transport Hh together with Ptc in motile puncta. Previous work from our laboratory described apical cytonemes that extend toward the A/P border from both A and P compartment cells (Ramirez-Weber and Kornberg, 1999). These cytonemes have motile, Dpp receptor-containing puncta and depend on Dpp expression (Hsiung et al., 2005; Roy et al., 2011). Basal cytonemes that also orient perpendicular to the A/P axis, but differ from the apical cytonemes in composition and

Development (2017) 144, 3134-3144 doi:10.1242/dev.149856

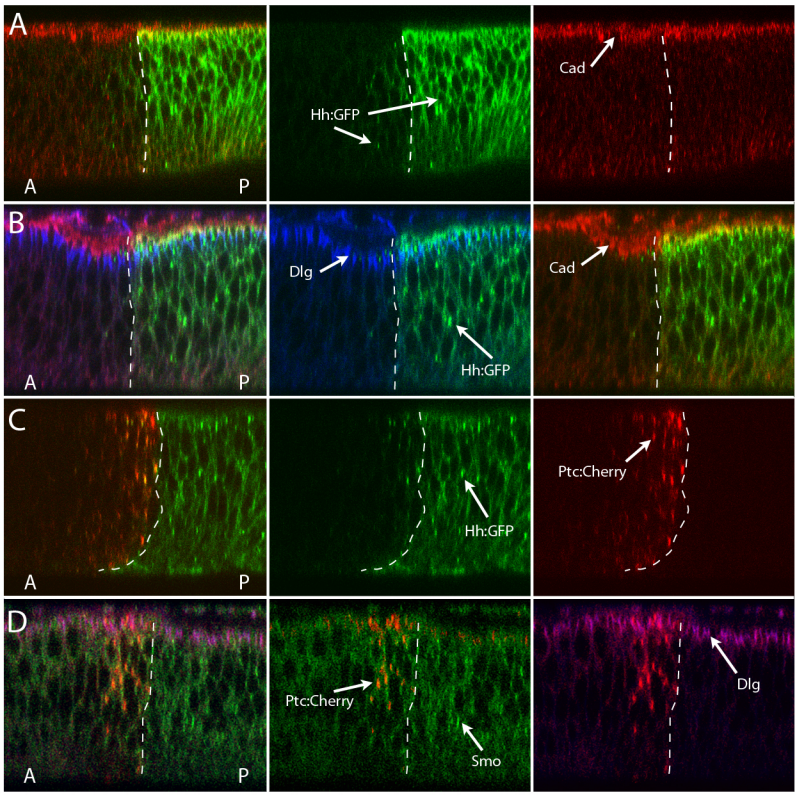

Fig. 6. Apicobasal distributions of Hh, Ptc and Smo in wing discs. (A-D) Sagittal images of BAC-encoded Hh:GFP, Ptc:mCherry and Smo:GFP. Dashed lines indicate the A/P compartment border. (A,B) Wing discs expressing Hh:GFP stained with α-Dlg (blue, B) and α-Cad (red, A,B). P compartment Hh:GFP was detected throughout basolateral membranes and overlapped with Cad- and Dlg-staining bands. A compartment Hh:GFP was membrane associated and extended to the Cad domain. (C) Ptc:mCherry puncta distributed along the apicobasal axis and colocalizing with Hh:GFP in the A compartment. (D) Ptc:mCherry was detected apically to the Dlg-staining domain (purple) and did not colocalize with Smo:GFP.

shape, were also described, but their function was not known. The Guerrero group has, more recently, shown that basal cytonemes traffic Hh (Bilioni et al., 2013; Bischoff et al., 2013; Callejo et al., 2011), giving further support to the idea that cells make multiple types of cytonemes that are tailored to specific signaling pathways (Roy et al., 2011).

The Guerrero group reported that basal cytonemes emanating from both A and P cells can be visualized with various membrane and cytoskeletal markers under conditions of Ihog overexpression (Bilioni et al., 2013; Bischoff et al., 2013; Callejo et al., 2011), and showed that several Hh pathway components mark cytonemes as well. Our observations with BAC-encoded Hh:GFP and Ptc:mCherry also suggest cytoneme-mediated trafficking that involves direct transfer of Hh to A compartment cytonemes. Colocalization of Hh and Ptc in the cytonemes suggests that Hh may bind directly to Ptc prior to arrival at the cell body of the A cell. The model of signal protein transfer that we favor is that uptake occurs at contacts that cytonemes make with target producing cells, and that signal transduction is temporally and physically separate from signal reception. Previous studies of Dpp signaling identified similar behaviors (Roy et al., 2014).

Cytonemes are required for the wing disc Hh gradient

We obtained evidence of an essential role for cytonemes in cells that lack either Dia, SCAR or Nrg function: mutant cells lacked basal cytonemes that normally extend posteriorly into the P compartment, and their Hh content was severely reduced, as was their level of Hh signaling. We also observed that A compartment cytonemes and Hh signaling are reduced in discs with P compartment cells deficient for the SNARE Syb. These phenotypes implicate A compartment cytonemes in Hh signaling and gradient formation, but they do not negate a role for P compartment cytonemes that deliver Hh to target A compartment cells. The Hh gradient is reduced after downregulation of SCAR, Pico, Flotillin 2 and the Capping proteins (Bischoff et al., 2013) in P compartment cells, indicating that cytonemes that extend anteriorly from the P compartment are also required. We do not have data to reconcile these findings, but we observed that under the conditions of Dia and SCAR depletion, some Hh was present in A compartment cells and these cells had a low level of signaling. It could be that the residual spread of Hh and the residual signaling is contributed by P compartment, cytoneme-mediated trafficking. This model posits that Hh transport and signaling are mediated both by cytonemes that extend from producing and from receiving cells. In addition, although cytonemes that take up signaling proteins have been observed to make direct contact with the cell bodies of target cells (Roy et al., 2014), the known properties of cytonemes are also compatible with cytoneme to cytoneme contacts. Further characterization of signaling protein movement should resolve the mechanisms involved.

The circuitous path from production to signal transduction

Histochemical analysis of a protein in fixed tissues can be used to provide precise information about steady-state distributions, but inferring kinetics is problematic without knowing the relative half-life or residence times for the protein in each location, or without knowing which stages might be rate limiting. For the Hh pathway in the wing disc, one of the key issues is to understand how Hh moves from P compartment cells in which it is made to the A compartment cells that it regulates. Antibody staining of normal L3 discs has revealed significant apical accumulation of Hh in both A and P compartment cells, and it was proposed that apical Hh release, spreading and uptake account for these distributions (Ayers et al., 2010). This model assumes that the route Hh takes between the apical domain of P cells to the apical domain of A cells is direct. However, the Guerrero group's discovery of a complex, circuitous path in P cells that involves endocytosis from the apical membrane,

Development (2017) 144, 3134-3144 doi:10.1242/dev.149856

encapsulation in vesicles, and basal translocation (Callejo et al., 2011) raises that possibility that Hh in the apical domain of A cells has also taken an indirect path, one that involves translocation after basal uptake (Kornberg, 2014). The analysis we report here supports this model of an indirect path in both A and P cells.

By following the evolving distribution of Hh:GFP expressed in a time-limited pulse, we found that Hh is initially apical in P compartment cells prior to its accumulation in the basal domain. This behavior is consistent with the Guerrero group's observations (Callejo et al., 2011). We also found that Hh:GFP taken up by A compartment cell cytonemes travels together with Ptc in vesicles that appear first in the basal domain, and that subsequent accumulations are more apical (Fig. 6). This choreography has hallmarks of sonic hedgehog (Shh) signaling in the vertebrate neural tube, where Shh is produced basal to the neural tube but signal transduction is localized to apical primary cilia (Chamberlain et al., 2008). We speculate that *Drosophila* Hh may also be targeted to specific apical locations for signal processing in A compartment cells, and it will be important to further characterize the intracellular localization of Hh relative to the other components of signal transduction to resolve the details of this process.

MATERIALS AND METHODS

BAC constructs and transgenesis

For Hh:GFP BAC, the 101.2 kb genomic insert in P[acman] clone CH321-61H05 (Venken et al., 2009) was reduced to 39.5 kb (chromosome 3R nucleotides 18950000 to 18989500) by recombineering (Venken et al., 2009), and sfGFP cDNA (Pedelacq et al., 2006) was inserted after the H254 codon. For Ptc:mCherry BAC, CH321-80E09 was recombineered to remove the *ptc* stop codon, and linker GGAGTG and mCherry cDNA were inserted. For Smo:GFP BAC, sfGFP cDNA was inserted after Ser33 in CH322-98K24. For Syb GRASP, GFP^{1-10} was fused in frame to the 3′ end of the *Syb* cDNA coding sequence and the chimera was inserted into pUAST.

Drosophila stocks

hh-Gal4, *hh*-nlsDsRed and *ptc*-Gal4 enhancer trap lines express in wing discs in patterns that mimic *hh* and *ptc*, respectively (Akimoto et al., 2005; Ramirez-Weber et al., 2000; Tanimoto et al., 2000). Stocks were obtained from Bloomington Drosophila Stock Center (BDSC): *UAS-disp* RNAi (#27247), *UAS-dia* RNAi (#28541), *tub*-$Gal80^{ts}$ (#7018), *UAS*-CD8:GFP (#5137), *yw*, *ubi*-RFP.nls FRT40A/CyO (#34500) and *UAS-Nrg* RNAi (#37496). *UAS*-CD8:mCherry (described in Roy et al., 2011); *UAS*-Hh:CD2 (described in Strigini and Cohen, 1997); and *UAS*-CD4:IFP2.0-T2A-HO1 (described in Yu et al., 2014). Stocks were also obtained from Vienna Drosophila Research Center (VDRC) Stock Center: *UAS-SCAR* RNAi (#21908) and *UAS-Syb* RNAi (102922KK). *dpp*-LexA *lexO*-CD4:GFP^{11} and *UAS*-CD4:GFP^{1-10} were provided by K. Scott (University of California, Berkeley, USA), and *lexO*-mCherryCAAX was provided by K. Basler (University of Zürich, Switzerland). All crosses were incubated at 25°C except for experiments with pulsed expression of UAS-*hh*:GFP or $Gal80^{ts}$-regulated expression of RNAi (4 h embryo collection at 25°C, 8 days at 18°C, and 36 h at 29°C for analysis of discs; for analysis of adults, incubation was at 25°C following the term at 29°C).

Immunochemistry

Wing discs were processed as described (Rao et al., 2015). Primary antibodies used were α-Ptc (1:200, Apa1, Developmental Studies Hybridoma Bank, DSHB), α-cleaved Caspase 3 (1:200, 9661, Cell Signaling Technology), α-DE-Cadherin (1:200, DECAD2, DSHB), α-Discs large (1:50, 4F3, DSHB) and α-Engrailed (1:100, 4D9, DSHB). Secondary antibodies (Invitrogen) used were goat α-mouse antibody (1:400, Alexa Fluor 555, 647), goat α-rabbit (1:400, Alexa Fluor 488) and donkey α-rat (1:400, Alexa Fluor 488).

Drosophila wing disc culture and imaging

Third instar wing discs were dissected in WM1 medium (Zartman et al., 2013) and placed in a chamber formed by double-sided 3M tape mounted on a glass slide and sealed with a coverslip. Live imaging was performed with a Nikon spinning-disc confocal microscope. Imaging of fixed samples was performed with a point laser confocal microscope (Leica SPE). GRASP analysis was conducted as described in Roy et al. (2014).

Cytoneme characterizations in mutant discs

To analyze Hh:GFP and Ptc gradients, projection images spanning the apicobasal axis were processed with Image J (maximal intensity). A P compartment area (100×40 µm area 10 µm from the A/P compartment border, marked by α-Ptc or mCherry expression) was quantified (Image J Plot Profile). Values were averages from eight discs.

Generation of clones lacking BAC-encoded Hh:GFP and time-limited pulsed expression of Hh:GFP

Mitotic clones not expressing BAC-encoded Hh:GFP were generated at L1 (hsFLP; *hh*:GFP FRT40A/*ubi*-RFP.nls FRT40A) by heat shock (37°C, 30 min). Expression of Hh:GFP was with *hh*-Gal4 *tub*-$Gal80^{ts}$ *UAS-hh*:GFP from a 2 h embryo collection incubated for 11 days at 18°C and for 24 h at 29°C.

Acknowledgements

We thank Chun Han, Xiaokun Shu, Carla Prat-Rojo, Enrique Martin Blanco, João Ortigao-Farias, Isabel Guerrero, the BDSC and the VDRC Stock Center for fly stocks; Koen Venken for recombineering advice; and members of the Kornberg laboratory for help and discussions.

Competing interests

The authors declare no competing or financial interests.

Author contributions

Conceptualization: W.C., H.H., R.H., T.B.K.; Methodology: W.C., H.H., R.H., T.B.K.; Validation: W.C., T.B.K.; Formal analysis: W.C., T.B.K.; Investigation: W.C., H.H., R.H.; Resources: H.H., R.H., T.B.K.; Data curation: W.C.; Writing - original draft: W.C.; Writing - review & editing: W.C., T.B.K.; Supervision: T.B.K.; Project administration: T.B.K.; Funding acquisition: T.B.K.

Funding

This work was funded by the National Institutes of Health (T32HL007731 to H.H.) and the National Institute of General Medical Sciences (GM030637, GM105987 and GM122548 to T.B.K.). Deposited in PMC for release after 12 months.

Supplementary information

Supplementary information available online at
http://dev.biologists.org/lookup/doi/10.1242/dev.149856.supplemental

References

Akimoto, A., Wada, H. and Hayashi, S. (2005). Enhancer trapping with a red fluorescent protein reporter in Drosophila. *Dev. Dyn.* **233**, 993-997.

Ayers, K. L., Gallet, A., Staccini-Lavenant, L. and Thérond, P. P. (2010). The long-range activity of Hedgehog is regulated in the apical extracellular space by the glypican Dally and the hydrolase Notum. *Dev. Cell* **18**, 605-620.

Bhattacharya, S., Stewart, B. A., Niemeyer, B. A., Burgess, R. W., McCabe, B. D., Lin, P., Boulianne, G., O'Kane, C. J. and Schwarz, T. L. (2002). Members of the synaptobrevin/vesicle-associated membrane protein (VAMP) family in Drosophila are functionally interchangeable in vivo for neurotransmitter release and cell viability. *Proc. Natl. Acad. Sci. USA* **99**, 13867-13872.

Bilioni, A., Sánchez-Hernández, D., Callejo, A., Gradilla, A. C., Ibáñez, C., Mollica, E., Carmen Rodriguez-Navas, M., Simon, E. and Guerrero, I. (2013). Balancing Hedgehog, a retention and release equilibrium given by Dally, Ihog, Boi and shifted/DmWif. *Dev. Biol.* **376**, 198-212.

Bischoff, M., Gradilla, A.-C., Seijo, I., Andrés, G., Rodríguez-Navas, C., González-Méndez, L. and Guerrero, I. (2013). Cytonemes are required for the establishment of a normal Hedgehog morphogen gradient in Drosophila epithelia. *Nat. Cell Biol.* **15**, 1269-1281.

Browne, E. N. (1909). The production of new hydranths in Hydra by the insertion of small grafts. *J Exp. Zool.* **7**, 1-23.

Burke, R., Nellen, D., Bellotto, M., Hafen, E., Senti, K.-A., Dickson, B. J. and Basler, K. (1999). Dispatched, a novel sterol-sensing domain protein dedicated to the release of cholesterol-modified hedgehog from signaling cells. *Cell* **99**, 803-815.

Callejo, A., Bilioni, A., Mollica, E., Gorfinkiel, N., Andrés, G., Ibáñez, C., Torroja, C., Doglio, L., Sierra, J. and Guerrero, I. (2011). Dispatched mediates Hedgehog basolateral release to form the long-range morphogenetic gradient in

the Drosophila wing disk epithelium. *Proc. Natl. Acad. Sci. USA*. **108**, 12591-12598.
Capdevila, J., Estrada, M. P., Sánchez-Herrero, E. and Guerrero, I. (1994a). The Drosophila segment polarity gene patched interacts with decapentaplegic in wing development. *EMBO J.* **13**, 71-82.
Capdevila, J., Pariente, F., Sampedro, J., Alonso, J. L. and Guerrero, I. (1994b). Subcellular localization of the segment polarity protein patched suggests an interaction with the wingless reception complex in Drosophila embryos. *Development* **120**, 987-998.
Chamberlain, C. E., Jeong, J., Guo, C., Allen, B. L. and McMahon, A. P. (2008). Notochord-derived Shh concentrates in close association with the apically positioned basal body in neural target cells and forms a dynamic gradient during neural patterning. *Development* **135**, 1097-1106.
Chin, A. C., Burgess, R. W., Wong, B. R. and Schwarz, T. L. (1993). Differential expression of transcripts from syb, a Drosophila melanogaster gene encoding VAMP (synaptobrevin) that is abundant in non-neuronal cells. *Gene* **131**, 175-181.
Denef, N., Neubüser, D., Perez, L. and Cohen, S. M. (2000). Hedgehog induces opposite changes in turnover and subcellular localization of patched and smoothened. *Cell* **102**, 521-531.
DiAntonio, A., Burgess, R. W., Chin, A. C., Deitcher, D. L., Scheller, R. H. and Schwarz, T. L. (1993). Identification and characterization of Drosophila genes for synaptic vesicle proteins. *J. Neurosci.* **13**, 4924-4935.
Feinberg, E. H., Vanhoven, M. K., Bendesky, A., Wang, G., Fetter, R. D., Shen, K. and Bargmann, C. I. (2008). GFP Reconstitution Across Synaptic Partners (GRASP) defines cell contacts and synapses in living nervous systems. *Neuron* **57**, 353-363.
Gordon, M. D. and Scott, K. (2009). Motor control in a Drosophila taste circuit. *Neuron* **61**, 373-384.
Gradilla, A.-C., González, E., Seijo, I., Andrés, G., Bischoff, M., González-Mendez, L., Sánchez, V., Callejo, A., Ibáñez, C., Guerra, M. et al. (2014). Exosomes as Hedgehog carriers in cytoneme-mediated transport and secretion. *Nat. Commun.* **5**, 5649.
Hsiung, F., Ramirez-Weber, F.-A., Iwaki, D. D. and Kornberg, T. B. (2005). Dependence of Drosophila wing imaginal disc cytonemes on Decapentaplegic. *Nature* **437**, 560-563.
Kicheva, A., Pantazis, P., Bollenbach, T., Kalaidzidis, Y., Bittig, T., Julicher, F. and Gonzalez-Gaitan, M. (2007). Kinetics of morphogen gradient formation. *Science* **315**, 521-525.
Kornberg, T. B. (2014). The contrasting roles of primary cilia and cytonemes in Hh signaling. *Dev. Biol.* **394**, 1-5.
Kornberg, T. B. and Roy, S. (2014). Communicating by touch–neurons are not alone. *Trends Cell Biol.* **24**, 370-376.
Lu, X., Liu, S. and Kornberg, T. B. (2006). The C-terminal tail of the Hedgehog receptor Patched regulates both localization and turnover. *Genes Dev.* **20**, 2539-2551.
Marigo, V., Davey, R. A., Zuo, Y., Cunningham, J. M. and Tabin, C. J. (1996). Biochemical evidence that patched is the Hedgehog receptor. *Nature* **384**, 176-179.
Matusek, T., Wendler, F., Polès, S., Pizette, S., D'Angelo, G., Fürthauer, M. and Thérond, P. P. (2014). The ESCRT machinery regulates the secretion and long-range activity of Hedgehog. *Nature* **516**, 99-103.
Mehta, A. D., Rock, R. S., Rief, M., Spudich, J. A., Mooseker, M. S. and Cheney, R. E. (1999). Myosin-V is a processive actin-based motor. *Nature* **400**, 590-593.
Miller, J., Fraser, S. E. and McClay, D. (1995). Dynamics of thin filopodia during sea urchin gastrulation. *Development* **121**, 2501-2511.
Muller, P., Rogers, K. W., Jordan, B. M., Lee, J. S., Robson, D., Ramanathan, S. and Schier, A. F. (2012). Differential diffusivity of Nodal and Lefty underlies a reaction-diffusion patterning system. *Science* **336**, 721-724.
Mullor, J. L., Calleja, M., Capdevila, J. and Guerrero, I. (1997). Hedgehog activity, independent of decapentaplegic, participates in wing disc patterning. *Development* **124**, 1227-1237.
Palm, W., Swierczynska, M. M., Kumari, V., Ehrhart-Bornstein, M., Bornstein, S. R. and Eaton, S. (2013). Secretion and signaling activities of lipoprotein-associated hedgehog and non-sterol-modified hedgehog in flies and mammals. *PLoS Biol.* **11**, e1001505.
Pédelacq, J.-D., Cabantous, S., Tran, T., Terwilliger, T. C. and Waldo, G. S. (2006). Engineering and characterization of a superfolder green fluorescent protein. *Nat. Biotechnol.* **24**, 79-88.
Pepinsky, R. B., Zeng, C., Wen, D., Rayhorn, P., Baker, D. P., Williams, K. P., Bixler, S. A., Ambrose, C. M., Garber, E. A., Miatkowski, K. et al. (1998). Identification of a palmitic acid-modified form of human Sonic hedgehog. *J. Biol. Chem.* **273**, 14037-14045.
Porter, J. A., Young, K. E. and Beachy, P. A. (1996). Cholesterol modification of hedgehog signaling proteins in animal development. *Science* **274**, 255-259.
Raftery, L. A., Sanicola, M., Blackman, R. K. and Gelbart, W. M. (1991). The relationship of decapentaplegic and engrailed expression in Drosophila imaginal disks: do these genes mark the anterior-posterior compartment boundary? *Development* **113**, 27-33.
Ramírez-Weber, F.-A. and Kornberg, T. B. (1999). Cytonemes: cellular processes that project to the principal signaling center in Drosophila imaginal discs. *Cell* **97**, 599-607.
Ramirez-Weber, F. A., Casso, D. J., Aza-Blanc, P., Tabata, T. and Kornberg, T. B. (2000). Hedgehog signal transduction in the posterior compartment of the Drosophila wing imaginal disc. *Mol. Cell* **6**, 479-485.
Rao, P. R., Lin, L., Huang, H., Guha, A., Roy, S. and Kornberg, T. B. (2015). Developmental compartments in the larval trachea of Drosophila. *Elife* **4**, e08666.
Roy, S., Hsiung, F. and Kornberg, T. B. (2011). Specificity of Drosophila cytonemes for distinct signaling pathways. *Science* **332**, 354-358.
Roy, S., Huang, H., Liu, S. and Kornberg, T. B. (2014). Cytoneme-mediated contact-dependent transport of the Drosophila decapentaplegic signaling protein. *Science* **343**, 1244624.
Sanders, T. A., Llagostera, E. and Barna, M. (2013). Specialized filopodia direct long-range transport of SHH during vertebrate tissue patterning. *Nature* **497**, 628-632.
Spemann, H. and Mangold, H. (1924). Über Weckung organisatorischer Fähigkeiten durch Verplanzung in organisatorische Umgebung. *Roux's Arch.* **109**, 557-577.
Stone, D. M., Hynes, M., Armanini, M., Swanson, T. A., Gu, Q., Johnson, R. L., Scott, M. P., Pennica, D., Goddard, A., Phillips, H. et al. (1996). The tumour-suppressor gene patched encodes a candidate receptor for Sonic hedgehog. *Nature* **384**, 129-134.
Strigini, M. and Cohen, S. M. (1997). A Hedgehog activity gradient contributes to AP axial patterning of the Drosophila wing. *Development* **124**, 4697-4705.
Tabata, T. and Kornberg, T. B. (1994). Hedgehog is a signaling protein with a key role in patterning Drosophila imaginal discs. *Cell* **76**, 89-102.
Tabata, T. and Takei, Y. (2004). Morphogens, their identification and regulation. *Development* **131**, 703-712.
Tanimoto, H., Itoh, S., ten Dijke, P. and Tabata, T. (2000). Hedgehog creates a gradient of DPP activity in Drosophila wing imaginal discs. *Mol. Cell* **5**, 59-71.
Taylor, A. M., Nakano, Y., Mohler, J. and Ingham, P. W. (1993). Contrasting distributions of patched and hedgehog proteins in the Drosophila embryo. *Mech. Dev.* **42**, 89-96.
Torroja, C., Gorfinkiel, N. and Guerrero, I. (2004). Patched controls the Hedgehog gradient by endocytosis in a dynamin-dependent manner, but this internalization does not play a major role in signal transduction. *Development* **131**, 2395-2408.
Toyoda, R., Assimacopoulos, S., Wilcoxon, J., Taylor, A., Feldman, P., Suzuki-Hirano, A., Shimogori, T. and Grove, E. A. (2010). FGF8 acts as a classic diffusible morphogen to pattern the neocortex. *Development* **137**, 3439-3448.
Venken, K. J. T., Carlson, J. W., Schulze, K. L., Pan, H., He, Y., Spokony, R., Wan, K. H., Koriabine, M., de Jong, P. J., White, K. P. et al. (2009). Versatile P[acman] BAC libraries for transgenesis studies in Drosophila melanogaster. *Nat. Methods* **6**, 431-434.
Yagi, R., Mayer, F. and Basler, K. (2010). Refined LexA transactivators and their use in combination with the Drosophila Gal4 system. *Proc. Natl. Acad. Sci. USA* **107**, 16166-16171.
Yamazaki, Y., Palmer, L., Alexandre, C., Kakugawa, S., Beckett, K., Gaugue, I., Palmer, R. H. and Vincent, J.-P. (2016). Godzilla-dependent transcytosis promotes Wingless signalling in Drosophila wing imaginal discs. *Nat. Cell Biol.* **18**, 451-457.
Yu, D., Gustafson, W. C., Han, C., Lafaye, C., Noirclerc-Savoye, M., Ge, W. P., Thayer, D. A., Huang, H., Kornberg, T. B., Royant, A. et al. (2014). An improved monomeric infrared fluorescent protein for neuronal and tumour brain imaging. *Nat. Commun.* **5**, 3626.
Zartman, J., Restrepo, S. and Basler, K. (2013). A high-throughput template for optimizing Drosophila organ culture with response-surface methods. *Development* **140**, 667-674.
Zeng, X., Goetz, J. A., Suber, L. M., Scott, W. J., Jr, Schreiner, C. M. and Robbins, D. J. (2001). A freely diffusible form of Sonic hedgehog mediates long-range signalling. *Nature* **411**, 716-720.
Zhou, S., Lo, W.-C., Suhalim, J. L., Digman, M. A., Gratton, E., Nie, Q. and Lander, A. D. (2012). Free extracellular diffusion creates the dpp morphogen gradient of the Drosophila wing disc. *Curr. Biol.* **22**, 668-675.

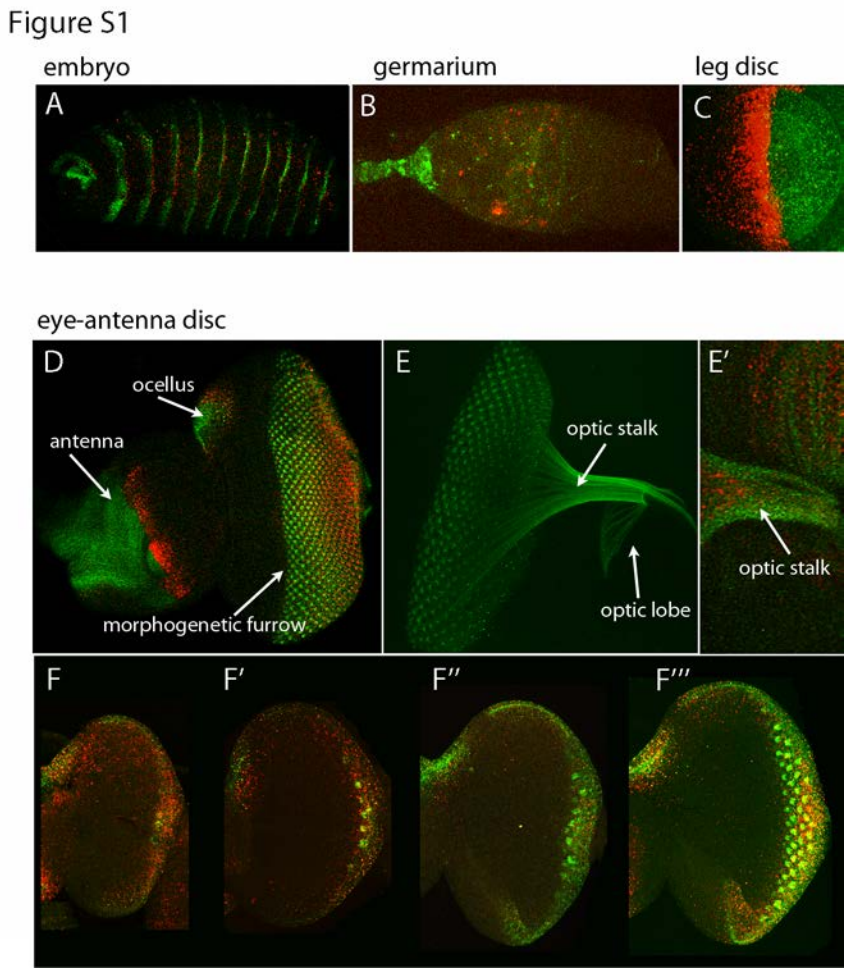

Figure S1. Distributions of Hh:GFP and Ptc:mCherry

Hh:GFP and Ptc:mCherry fluorescence in preparations of a late stage embryo (A), germarium (B), L3 leg disc (C), L3 eye-antennal disc (D-F"'). (F-F"') Successively later stages of early L3 eye disc showing increase in number of ommatidial clusters. Scale bars: (A) 100 μm; (B) 10 μm

Figure S2

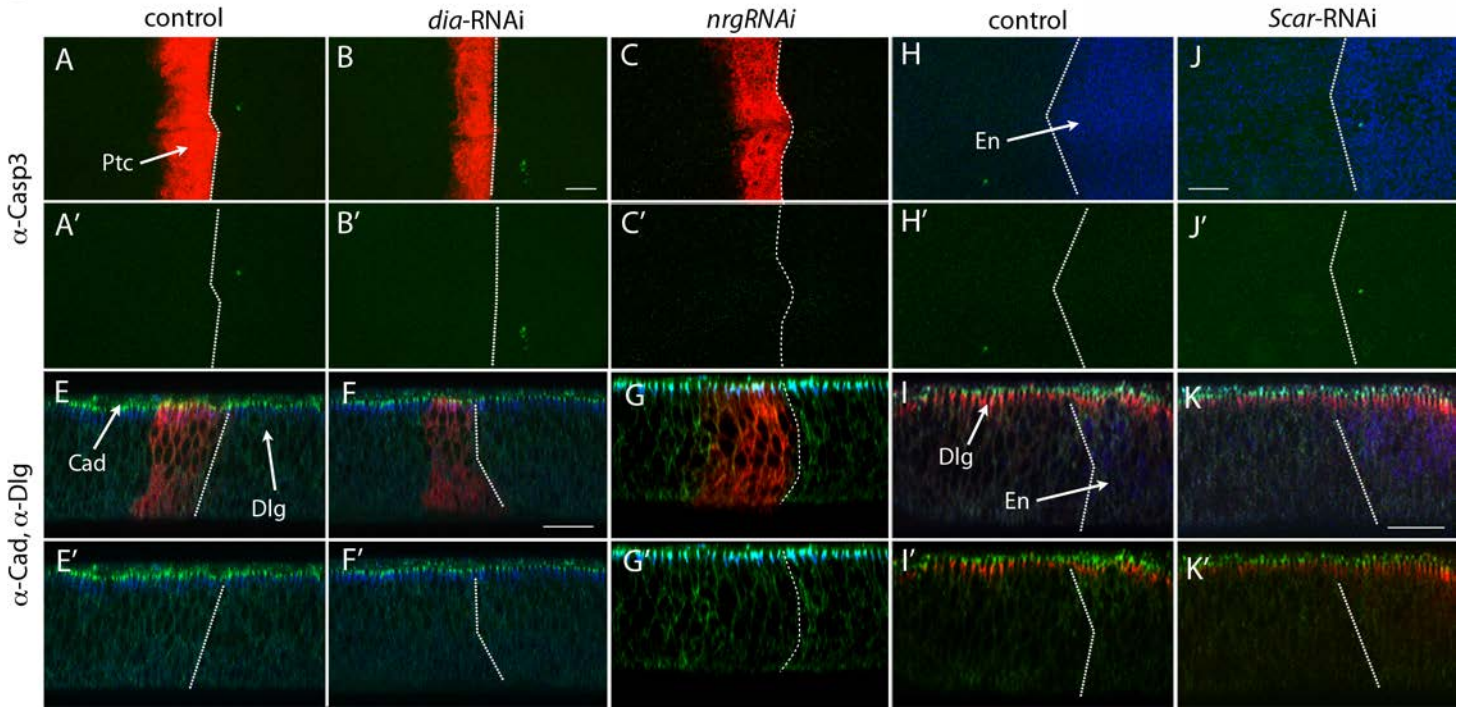

Figure S2. Neither cell death nor apicobasal polarity affected by expression of *dia*RNAi, *Scar*RNAi and *nrg*RNAi

(A,C,E,G,I) Frontal images of the pouch region of late L3 wing discs with dying cells marked with α-cleaved Caspase 3 staining (green); *ptc* domain (red); posterior compartment marked with α-Engrailed (blue). (B,D,F,H-J') Sagittal images of the pouch region of late L3 discs marked with α-Cad2 (green); α-Discs large (blue in B,D,F; red in H,J); *ptc* domain (red in B,D,F); posterior compartment marked with α-Engrailed (blue in H,J). Genotypes: (A-D) *ptc*-Gal4 *tub*-Gal80^{ts} *UAS*-CD8:mCherry *UAS-dia*RNAi; (E,F) *ptc*-Gal4 *tub*-Gal80^{ts} *UAS*-CD8:GFP *UAS-nrg*RNAi; (G-J) *ptc*-Gal4 *tub*-Gal80^{ts}*UAS-Scar*RNAi. (A,B,G,H) incubated at 18°C; (C-F,I,J) incubated at 18°C for approximately eight days followed by incubation at 29°C for 24-36 hrs prior to dissection. Dotted lines mark the A/P boundary. Scale bars: 20 μm.

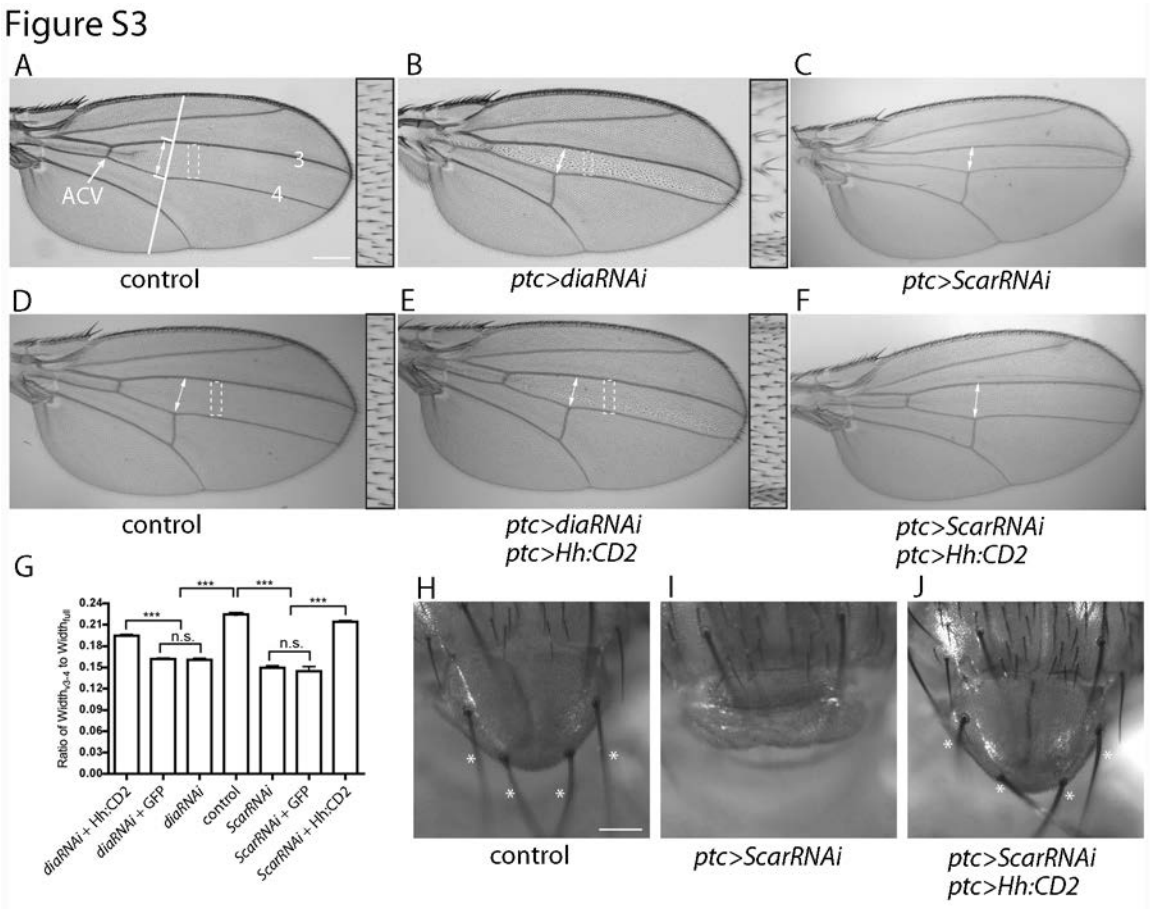

Figure S3. Wing blade and scutellum morphology of *dia*- and *Scar*-depleted flies

(A-F) Images of wings show that depletion of Dia and Scar in the *ptc* domain reduces Hh signaling. The intervein region between veins 3 and 4 (marked by double sided arrows) was reduced and the anterior cross vein (ACV) was absent in wings depleted for Dia (*ptc*-Gal4 *UAS*-Gal80^{ts} *UAS-dia*RNAi (B) or Scar (*ptc*-Gal4 *UAS*-Gal80^{ts} *UAS-Scar*RNAi (C) compared to control (A). The density of hairs in Dia-depleted wings was less that control (see high magnification insets of region boxed by dashed white line). Expression of CD2:Hh did not affect control wings (D) (*ptc*-Gal4 *UAS*-Gal80^{ts} *UAS*-Hh:CD2), but restored the 3-4 intervein region to normal size in Dia- and Scar-depleted wings (*ptc*-Gal4 *UAS*-Gal80^{ts} *UAS-dia*RNAi *UAS*-Hh:CD2 (E); *ptc*-Gal4 *UAS*-Gal80^{ts} *UAS-Scar*RNAi *UAS*-Hh:CD2 (F). Hair density in *dia*-depleted wings was also restored (E). (G) Bar graph showing normalized size of 3-4 intervein region in control and mutant wings. n=11 for all genotypes except n=10 for (D). The symbol (***) denotes P<0.001, two-tailed t-test; Bar value shown as mean ± s.d. (H-I) Depletion of *Scar* reduces the scutellum (I), but expression of Hh:CD2 (J) restores both scutellum morphology and the four scutellar macrochaetes (*) to normal (H). Genotypes are as in (A, C, F). Incubation was at 18°C for 8 days after egg laying, 29°C for 36 hrs, and 25°C until eclosion. Scale bars: (A) 200 μm; (H) 100 μm.

Movie 1. Cytoneme extension and retraction

Cytonemes from A compartment cells marked with membrane-tethered Cherry (*ptc*-Gal4 *UAS*-CD8:Cherry) orient towards the P compartment in the hinge region of this late 3rd instar wing disc. Their dynamic extension and retraction is recorded in this movie, which was taken at 12 second intervals in a 10 min period and is shown at 10 frames/second.

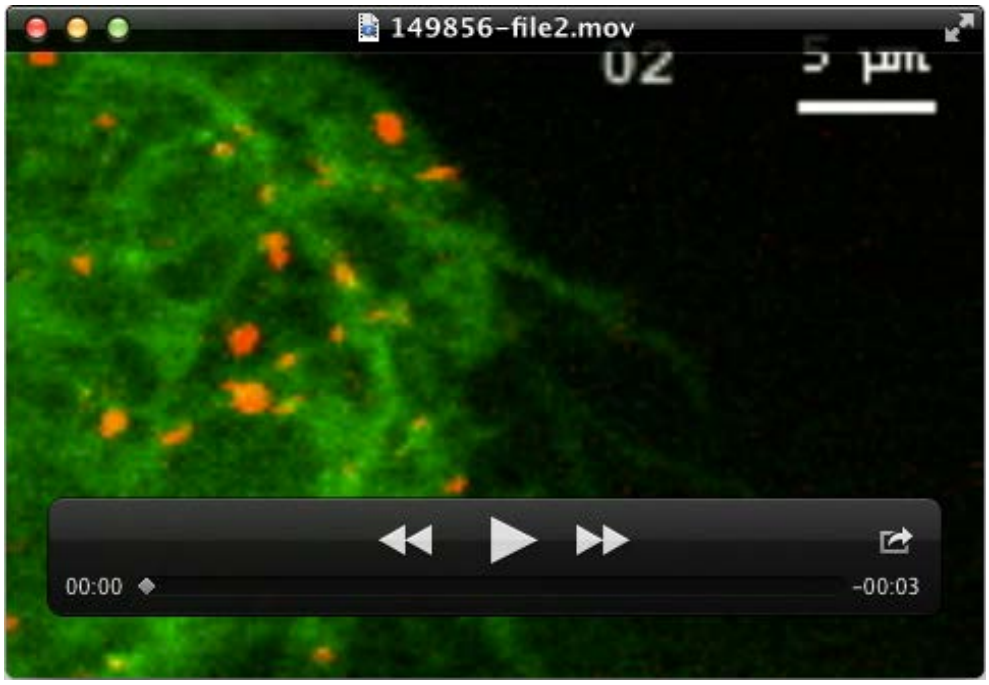

Movie 2. Ptc moves along cytonemes

BAC-encoded Ptc:mCherry marks motile puncta that travel in anterograde and retrograde directions along cytonemes that extend from A compartment cells marked with CD8:GFP (*ptc*-Gal4 *UAS*-CD8:GFP). The video was taken at the hinge region of a late 3rd instar wing disc; images were acquired every 15 seconds during an 8 min period and are shown at 10 frames/second.

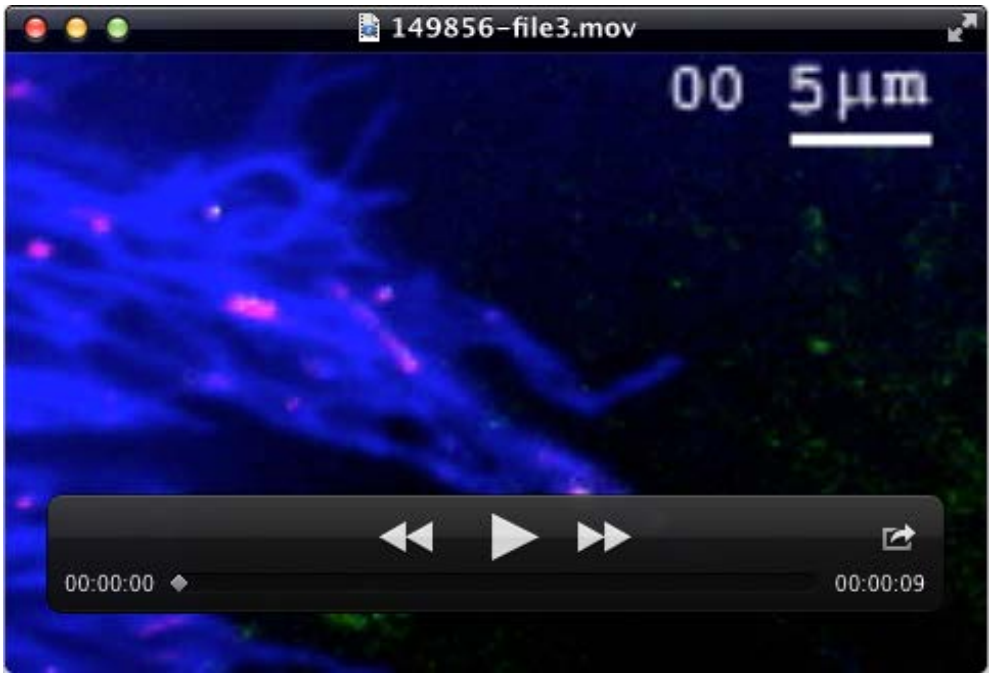

Movie 3. Hh and Ptc colocalize in cytoneme-associated motile puncta

Puncta containing BAC-encoded Hh:GFP and BAC-encoded Ptc-mCherry move in cytonemes marked with CD4:IFP2.0-HO1 (*ptc*-Gal4 *UAS*-CD4:IFP2.0-HO1; blue) that extend from A compartment cells in the hinge region of a late 3rd instar wing disc. Movement is in a net retrograde direction towards the A compartment. Pictures were taken every 4 seconds during a 6.5 min period and are shown at 10 frames/second.